

# A full disk image standardisation of the synoptic solar observations at the Meudon Observatory

V.V. Zharkova<sup>1</sup>, S.S. Ipson<sup>1</sup>, S.I. Zharkov<sup>1</sup>, A. K. Benkhalil<sup>1</sup> and J. Abouadarham<sup>2</sup>,

<sup>1</sup> Department of Cybernetics, Bradford University, Bradford BD7 1DP, UK

<sup>2</sup> LESIA, The Paris-Meudon Observatory, F92195 Meudon Principal Cedex, FRANCE

## ABSTRACT

The paper presents techniques developed for an automated image standardisation including limb fitting, removal of geometrical distortion, size standardisation and intensity normalisation. The limb fitting starts with an initial estimate of the solar centre using raw 12-bit image data and then applies a Canny edge-detection routine. Candidate edge points for the limb are selected using a voting method and the chosen points fitted to a quadratic function by minimising the algebraic distance using SVD. The corrected images are generated using nearest neighbour, bilinear or bicubic interpolation. Because of a limb darkening and variation in the atmosphere visibility over the solar disc the image intensity renormalisation is also required. This is achieved by fitting a background function in polar coordinates to a set of sample points having the median intensities and by standardising the average brightness. The research is done for the European Grid of Solar Observations (EGSO) project.

## 1. INTRODUCTION

This paper describes the automated pre-processing techniques which have been developed for a wide range of solar images. They have been tested on many images from the Meudon Observatory as well as some from other observatories. The pre-processing operations generally applied to solar images include correcting the shape of the Sun which may be elliptical in the raw captured image and correcting (cleaning) the large scale variation of intensity over the solar disk caused by non-uniform illumination. This effect is radially symmetric

and greatest near the limb. Apart from making corrections to the images in order to make a subsequent analysis more accurate and reliable, the pre-processing may also be used to identify images which have been corrupted in some way so that they can be rejected as unsuitable for further processing. A collection of archived images from the Meudon observatory is shown in Figure 1 illustrating a range of the image characteristics defined from observations. The images differ in the numbers and sizes of prominences appearing on the limb, the intensity of off-disk background illumination and the occasional presence of linear features which may be broad or narrow. Although the image header files contain information on the position and size of the solar disk, this information is generally not precise, the discrepancies, amounting to several pixels, varying in magnitude from image to image

The pre-processing methods are either semi-interactive [1] or adjusted to the images of a particular type from a particular observatory [2-4]. In the more general case of limb fitting with a wider range of solar images, problems can be caused by complex shapes of limb edges. This may result in a wide range of magnitudes of edge gradient and sometimes in the lack of a unique point of inflection. Selecting the edge points to be used in the curve fitting routine is complicated in general, by a presence of prominences on the limb and edge features inside the limb. Ellipse fitting routines vary in complexity and reliability, and only Walton et al (1998) [3] specified the method used and only the approach of Veronig et al (2001) [4] takes into account possible non-radial illumination effects.

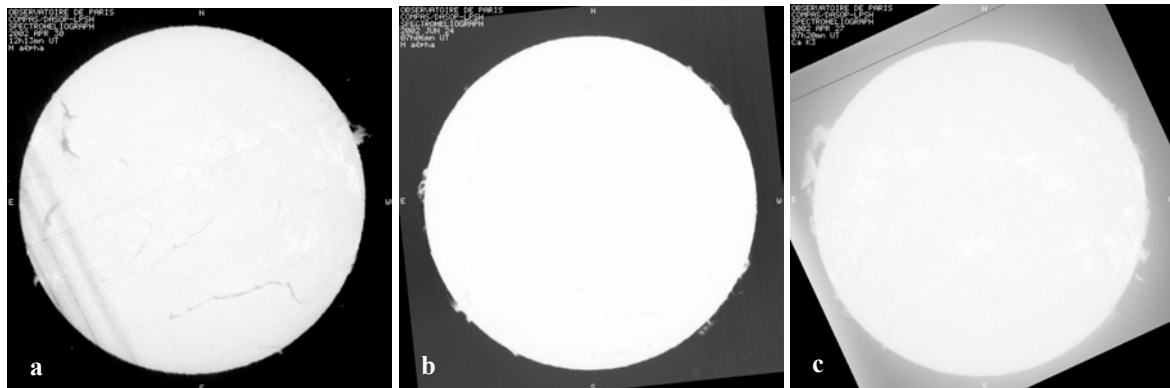


Figure 1. Possible variations in image characteristics from the full-disk H $\alpha$  and Ca K solar images (Meudon) revealing the non-radial dark lines (a), image legend and prominences (b-c), brighter image background (c)

In this paper some image pre-processing techniques are present which automatically determine a limb shape and solar centre in order to identify and remove non-uniform

illumination effects. They have been applied to a number of H $\alpha$  and Ca II K1 (wing of line) and Ca II K3 (centre of line) full-disk solar images captured on a

photographic film at the Meudon Observatory and scanned to a resolution of about  $900 \times 900$ .

## 2. IMAGE CLEANING TECHNIQUES

### 2.1 Limb fitting and geometrical correction

The solar images from the Meudon Observatory were digitized to the 12 bit with solar diameters of about 800 pixel. Superimposing circles on the images using the solar radius and centre information provided in the file headers showed that the solar disks were generally elliptical with a difference of about 1% between major and minor axes and with errors, often of several pixels, in the position of the centre indicated in FITS headers. It was decided therefore to determine the actual sizes and centres of the solar disks and in each case correct the disk to a circular shape of diameter 840 pixel centred in an image of size  $1024 \times 1024$  pixel.

#### 2.1.1 Limb fitting

The method used to fit an ellipse to the limb of the Sun is described in details in the paper Zharkova et al (2002) [5]. Similar to the methods mentioned in the introduction, an initial approximation of the disk centre and radius is first computed. This is followed by edge-detection using the Canny Edge Detection algorithm [6] and the selection of candidate points for fitting to an ellipse using information from the initial estimate. The candidate limb points are then fit to an ellipse using a least square deviation approach, iteratively removing points which are off the limb.

The fit is performed interactively, removing the outliers with the biggest radial errors after the previous fit, until a standard deviation of radial distance between the points and the fitted ellipse is less than 0.75 pixel.

#### 2.1.2 Geometrical correction of the solar shape

Having determined the elliptical shape of a solar limb, a single transformation combining all the geometrical corrections should be applied in order to correct the shape back to a circle before applying the limb darkening corrections (for details see Zharkova et al, 2002 [5]). Applying the individual transformations using a sequence of the rotation and rescaling operations will result in a build up of interpolation errors. The transformation applied should reverse the process that caused the distortion. In the case where the distortion is a stretching in a particular direction, the transformation combines the following steps: a translation to move the centre of co-ordinates to centre of ellipse; a rotation to make the principal axes of ellipse parallel to the image edges; a rescaling in the horizontal and vertical directions to make the major and minor axes of the Sun the same required size; the inverse rotation; a translation to move the centre of the Sun to the centre of new image. The geometrical transformation from a new image to the original image determines the point in the latter from which a particular pixel in the new image

came, and its value can be obtained by a nearest neighbour, bilinear or bi-cubic interpolation.

#### 2.1.3. The results

Figure 2 shows an example of applying these procedures to a solar image from Meudon Observatory: (a) is the original  $H\alpha$  image; (b) - the ellipse fitted to the limb points initially selected which include parts of prominences while only the edge points lying between the two circles obtained from analysis of a distance histogram are used in the fit; (c) shows the ellipse fitted to the final set of limb points when the standard deviation of the distance between edge points and ellipse is less than 0.75 pixel; (d) presents the final image corrected in size and shape. In the case of this Meudon image, the distortion from circular shape is about 8 pixels in 800 pixels. Repeating the process, the resulting ellipse fit is generally within about a tenth of a pixel of the corresponding standardized values giving a good indication of the consistency and accuracy of the procedure.

### 2.2 Intensity correction

The second step in the cleaning procedure is to correct the intensity variation of the standardized images by dividing them by an estimated average background image (see for details Zharkova et al, 2002 [6]). The intensity correction assumes that flat fielding corrections have been applied to the raw images at the observatories and ignores a possibility of the non-radial background illumination.

#### 2.2.1 Details of the method

The first stage is to map the standardized image from Cartesian coordinates to polar coordinates. Figure 3 shows the original (a) and transformed version (b) of the  $H\alpha$  image. Background images, computed using the median method, are used to correct the intensity of the original image for limb darkening. The median value of each row was calculated and used to replace the intensity in each row. The new rectangular image corresponding to Figure 3(b) is shown in Figure 4(a) and transformed back to Cartesian co-ordinates, as shown in Figure 4(b) for a use in limb darkening correction of the original images. The use of the median is seen to be a very effective way of removing local details. All features have to be removed from the image in order to create the background image. This can be difficult without also removing some of the background non-uniform illumination if the background illumination is not radially symmetric.

#### 2.2.2 Intensity correction results

Figure 5 shows an  $H\alpha$  image corrected for radian intensity illumination by dividing by the corresponding median estimated background image, and rescaled to a standard normalization. The figure shows the original image, the corrected image and an intensity profile at the position of the line superimposed on the solar image.

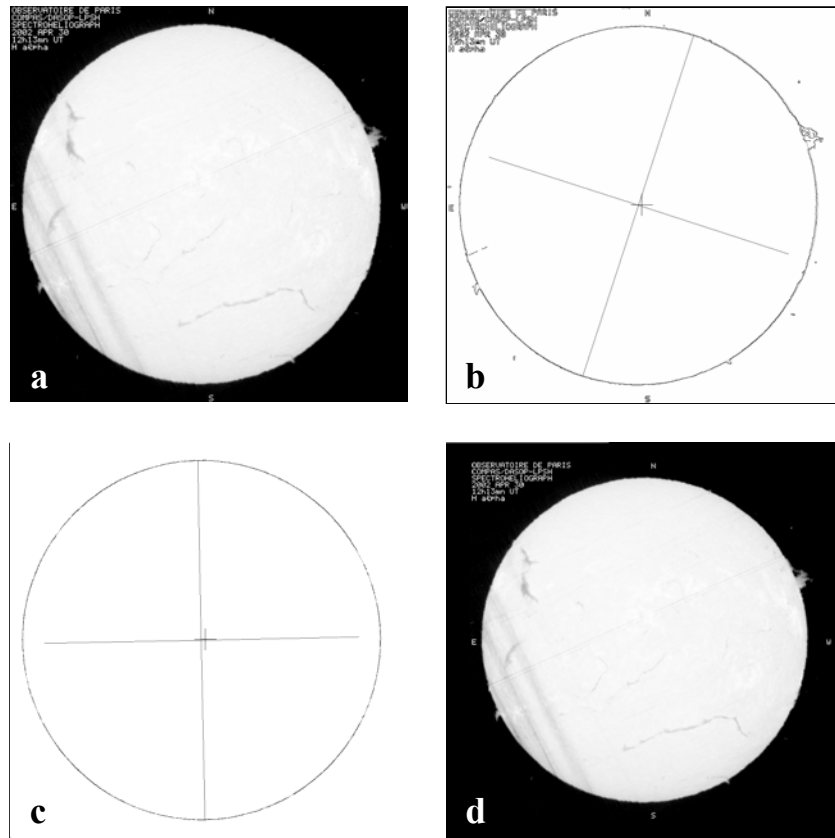


Figure 2. Limb fitting and image standardization stages; (a) original image, (b) initial ellipse fit, (c) refined ellipse fit (d) Standardized image after a geometrical correction. The small cross near the centre of (b) and (c) indicates the position of the initial estimate of the disk centre while the large cross indicates the orientation and centre of the ellipse fitted to the edge points in the figure.

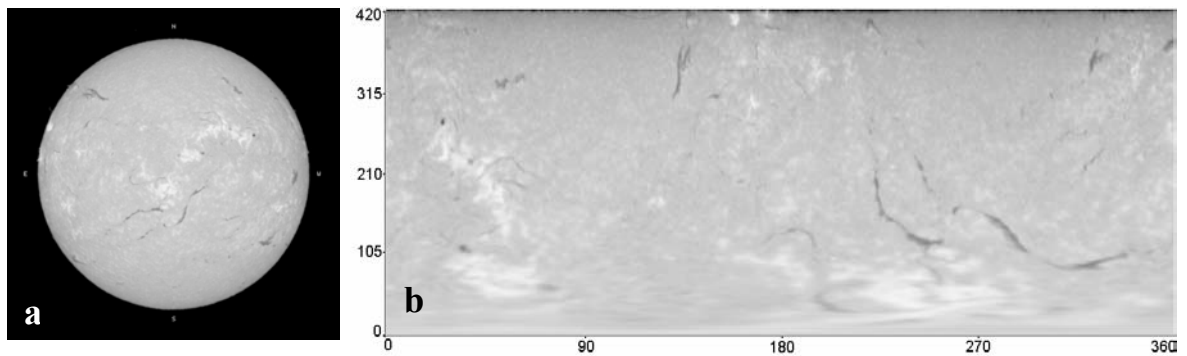


Figure 3. (a) Original H $\alpha$  image, (b) Image mapped to polar coordinates.

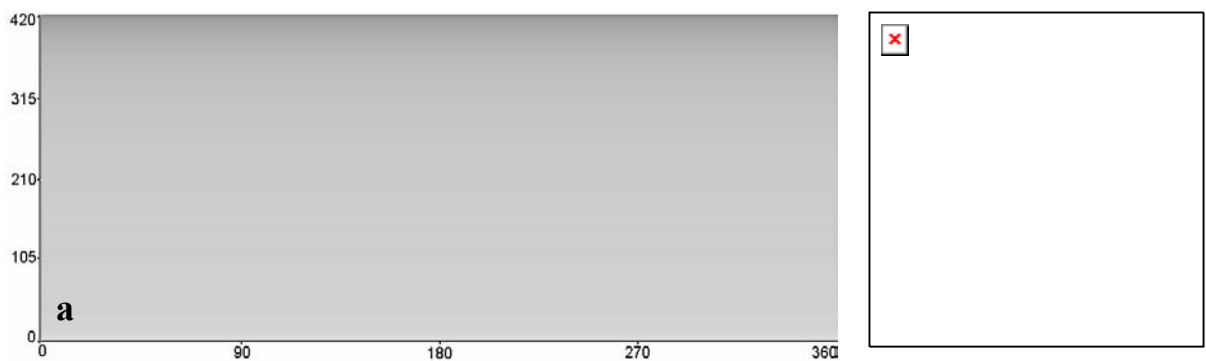


Figure 4. (a) Estimated background illumination obtained by replacing each row of image in 3(b) by its median value, (b) Estimated background image for image 3(a) obtained by mapping image 4(a) from polar to Cartesian co-ordinates.

### 3. CONCLUSIONS

The procedures developed for limb fitting using the Canny edge detector depend on general properties of the images which have been found remain valid over all the images tested despite in some cases the procedures have to be iterated. Repeating the procedure on corrected images, values of centre position and radius returned are found to be generally within about one tenth of a pixel of the standard values. Once the centre of the solar disk and its radius has been found, a radial limb darkening correction can be applied

using a standard form if the intensity is calibrated. Otherwise, most authors have found that estimating the limb darkening using the medians of concentric rings of pixels gives the best results and we have found the same.

### ACKNOWLEDGEMENTS

This work has been supported by the European Commission under the European Grid for Solar Observations, project IST – 2001 – 32409.

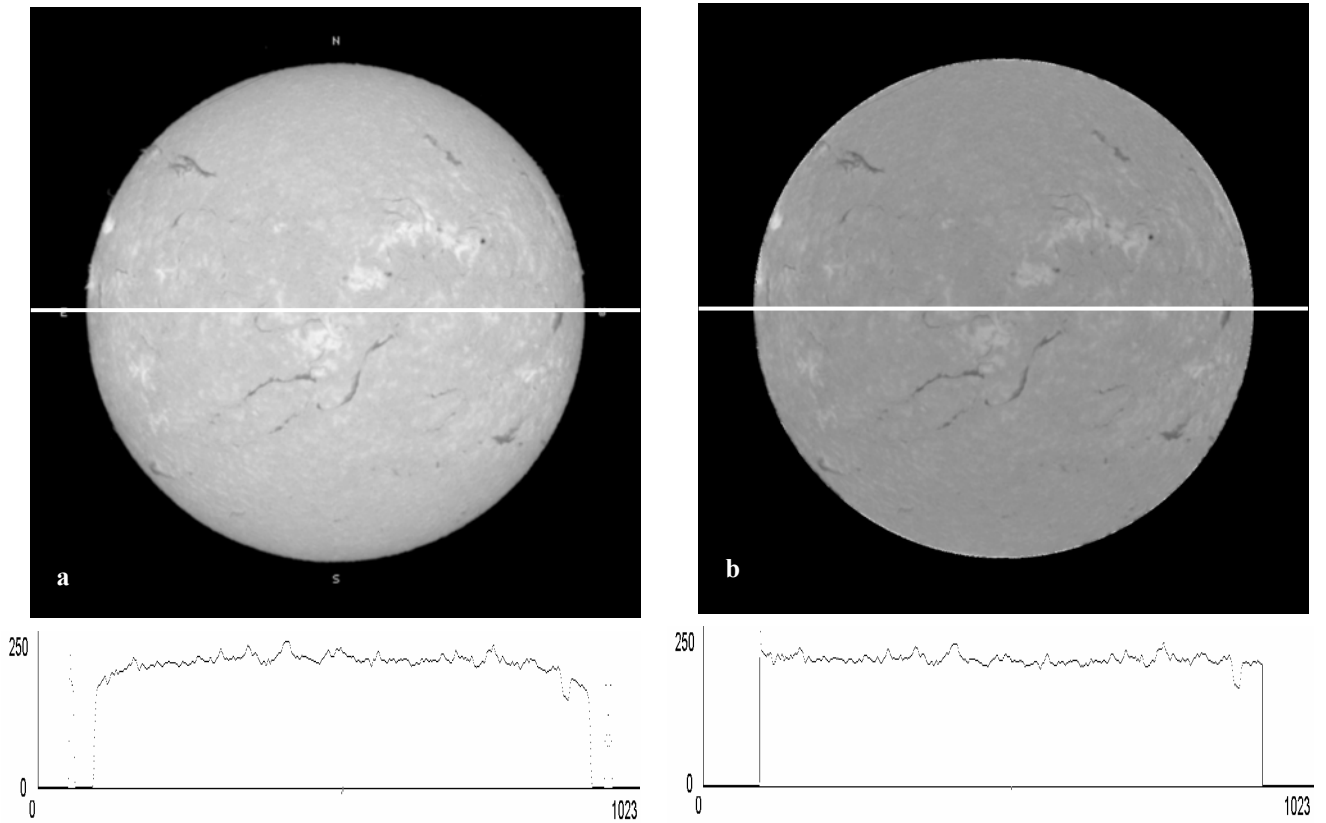


Figure 5. (a) Original H $\alpha$  image, (b) H $\alpha$  image corrected using median of rows of polar image, with plots of the intensities along the horizontal lines drawn through the images shown at the bottom.

### REFERENCES

1. C. Kohl, R. Lerner, A. Hough, C. Loisel, J. Dolan, M. Friedman, and M. Roubentchik, 1994 Proc. DARPA Image Understanding Workshop, Monterey, CA, pp. 13-16, November, 1994.
2. C. Denker, A. Johannesson, P. R. Goode, W. Marquette, H. Wang, H. Zirin, *Solar Physics J*, Volume 184, pp. 87-102, 1998
3. S. R. Walton, G. A. Chapman, A. M. Cookson, J. J. Dobias, and D. G. Preminger, *Solar Physics J*, v. 179, Issue 1, pp. 31-42, 1998.
4. A. Veronig, M. Steinegger, W. Otruba, A. Hanslmeier, M. Messerotti, M. Temmer, S. Gonzi, and G. Brunner, *Hvar Obs. Bull.* 24, pp. 195–205, 2001.
5. V.V.Zharkova, S.I.Ipson, S.I.Zharkov, A. Benkhalil and J.Abouadarham, *Solar Physics*, 2002, (submitted).
6. J. Canny, *IEEE Transactions on Pattern Analysis and Machine Intelligence*, PAMI-8(6): pp. 679-698, 1986.